Journal of Digital Food, Energy & Water Systems [JD-FEWS]

JDFEWS 5 (2): 65 - 82, 2024
ISSN 2709-4529

Predictive simulation of groundwater contamination due to landfill leachate: A case study on the Robinson Deep Landfill, Johannesburg, South Africa

Osman Abdullahi OSMAN
[1]Department of Civil Engineering, Vaal University of Technology, South Africa
othmanaom@gmail.com

George Mathews OCHIENG
[1]Department of Civil Engineering, Vaal University of Technology, South Africa

Sophia RWANGA
[2]University of Johannesburg, Department of Civil Engineering, South Africa

Received: 15 November 2024
Review: 11 December 2024
Accepted: 13 December 2024
Published: 16 December 2024

Abstract - Groundwater contamination from municipal solid waste landfills is a global issue, including in South Africa. The Robinson Deep landfill (RDL) in Johannesburg needs more leachate collection and handling facilities, has a shallow groundwater table, and no groundwater quality forecast tool. This situation poses a risk of groundwater contamination. This study aimed to construct groundwater flow and contaminant transport models to predict contamination from leachate migration at RDL. Visual MODFLOW Flex (VMOD-Flex) software was used for model construction and verification. Heavy metal concentration observations of Aluminium (Al), Cadmium (Cd), Manganese (Mn), and Lead (Pb) from boreholes BH-1, BH-2, BH-3, and BH-H near the RDL were used to calibrate and validate the contaminant transport model (CTM). The result of the CTM predictive simulations for 2030 show that Mn and Pb concentrations in the BH-H groundwater could reach 4.28 mg/L and 6.85 mg/L, respectively, exceeding permissible limits of 0.01 mg/L for Pb and 0.4 mg/L for Mn. The simulations indicate that the RDL threatens groundwater quality, especially in the northern areas of the landfill. Based on these findings, a recommendation is made for future studies on assessing and modelling groundwater quality to focus on areas where increased concentrations of Pb and Mn are predicted. Further, it is recommended that precautionary preventive measures be implemented to mitigate possible contamination of groundwater in the northern areas of the landfill.

Keywords: *Predictive simulation, groundwater contamination, transport modelling, landfill leachate, Robinson Deep landfill.*

JDFEWS 5 (2): 65 - 82, 2024
ISSN 2709-4529

1. Introduction

Groundwater is a globally valued commodity hidden from human eyesight. This invaluable resource only sometimes gets the requisite protection it deserves comparable to its usefulness to human needs [1]. Groundwater contamination has been reported in every global community, from the most developed nations, such as Norway and Switzerland [2], to the least developed countries [3][4]. Although groundwater contamination occurs due to different natural and anthropogenic factors, contamination in the proximity of municipal solid waste landfills (MSWLFs) has been reported in South Africa [5][6][7][8][9][10]; and many parts of the world [2][3][11][12][13][14]. MSWLFs release a liquid waste called 'leachate' that is 'leachate' rich in heavy metals and other emerging contaminants such as Polychlorinated Biphenyls [14]. The stated contaminants are due to a combined effect and presence of soil moisture, rainwater infiltration, groundwater seepage, surface water penetration, low pH in early landfill stages, and biochemical and biomechanical waste degradation [15]. The situation necessitates understanding groundwater flow through modelling systems, monitoring, and implementing protective measures to safeguard this invaluable resource from contamination.

Generally, a model is a simplified representation of a real system, a portion of the complex natural world. Models assist in understanding systems and evaluating management scenarios that cannot be tested in full-scale format [16]. Like any other model, a groundwater model is a simplified version of complex reality, and it simulates spatial and temporal properties of a real groundwater system or one of its parts physically (for example, laboratory sand tank) or mathematically [16][17]. A mathematical groundwater flow model describes the physical processes and boundary conditions of a particular groundwater flow problem, which can be solved deterministically using either an analytical approach if the problem is simple or numerical approaches capable of solving more complex groundwater flow problems [18]. Numerical methods are the best choice for approximate solutions for groundwater flow and contaminant transport problems [19]. According to Kumar [20], the finite difference method (FDM) based numerical models have prevailed in the hydrogeological practice in both academia and industry, and the most prominent FDM-based groundwater modelling program is the modular three-dimensional finite-difference groundwater flow model (MODFLOW) [21]. [22] used MODFLOW and the parameter estimation tool (PEST [23]) within the graphical user interface Visual MODFLOW to construct and calibrate groundwater flow models of a large area in central Limpopo, South Africa. [24] used the multispecies transport model (MT3DMS [25]) to model the groundwater quality of the Atlantis aquifer near Cape Town, South Africa. [26] used MT3DMS to simulate contaminant transport at a sewage farm in Tamil Nadu, India. Both studies [24] and [26] used MODFLOW, MT3DMS, and PEST to construct, calibrate, validate, and perform predictive simulations with their groundwater flow and transport models.

In previous studies of the Robinson Deep landfill (RDL), [8] identified that groundwater monitoring boreholes of the RDL showed higher concentrations of contaminants, including several types of flame retardants. [27], a study of the RDL reports a need for a formally installed landfill liner system at the base of the RDL. [5] and [8] reported that in the case of the RDL, a geosynthetic clay liner system was installed, covering only a portion of the landfill site. From the findings of previous studies on the RDL, it can be inferred that the groundwater beneath the RDL is vulnerable to contamination. [28] corroborated these findings that groundwater beneath the RDL is vulnerable to contamination due to the shallow water table and a lack of groundwater quality forecast tools that can be utilised to develop a proper groundwater management and protection schedule for the RDL and its impacted areas.

From the preceding, it is evident that urgent measures must be implemented to protect groundwater resources in the RDL and its proximate area. In this regard, we opted for this study to apply current technology as a tool to assess groundwater conditions at the RDL. Given the importance and effectiveness of numerical groundwater flow and transport models, groundwater flow and contaminant transport models were set up for the RDL and its proximate area using Visual MODFLOW Flex-8.

This study aims to establish a calibrated groundwater flow and contaminant transport model for the RDL area to predict groundwater quality in and around the RDL. The study's findings may support the landfill's post-closure care so that landfill managers and the government can ensure that this landfill safely stabilises without damaging groundwater quality.

JDFEWS 5 (2): 65 - 82, 2024
ISSN 2709-4529

2. Methodology

2.1. Study area description

The study area (RDL and its proximity) is in Johannesburg South, Gauteng Province, South Africa (Figure 1). It encloses an area of 10.08 km^2 that falls under the geographic coordinates of -26.229385S, 28.020817E, and -26.260264S, 28.051153E (Datum: WGS 84).

According to the Johannesburg hydrogeology map, the RDL is in sandy-loam-sandy-clay-loam soil type [29]. The location implies that the area may have slower groundwater movement. In addition, geological maps, including the Geology of Johannesburg, Geological Series-West Rand 2626, Geological Series-East Rand 2628, and the Simplified Geological Map of South Africa and the Kingdoms of Lesotho and Swaziland [30][31][32][33] show some areas where rocks belonging to the Wit-Waters-Rand supergroup are exposed to the surface. These areas may allow a reduced groundwater recharge rate owing to the need for secondary porosity.

The aquifer systems in the study area consist of a shallow Karoo aquifer, a deep Karoo aquifer, and a deeper Wit-Waters-Rand aquifer. The shallow aquifer is considered unconfined to confined; the deep aquifer is confined [34]. Deep and confined aquifers tend to be protected against leachate plumes that migrate from Municipal Solid Waste Landfills (MSWLs). In addition, it is likely that shallow and deep aquifers exchange contaminants if hydraulically connected [35].

This study aimed to construct groundwater flow and contaminant transport models to predict groundwater contamination due to leachate migration from the RDL. The materials and methods are described in the next section.

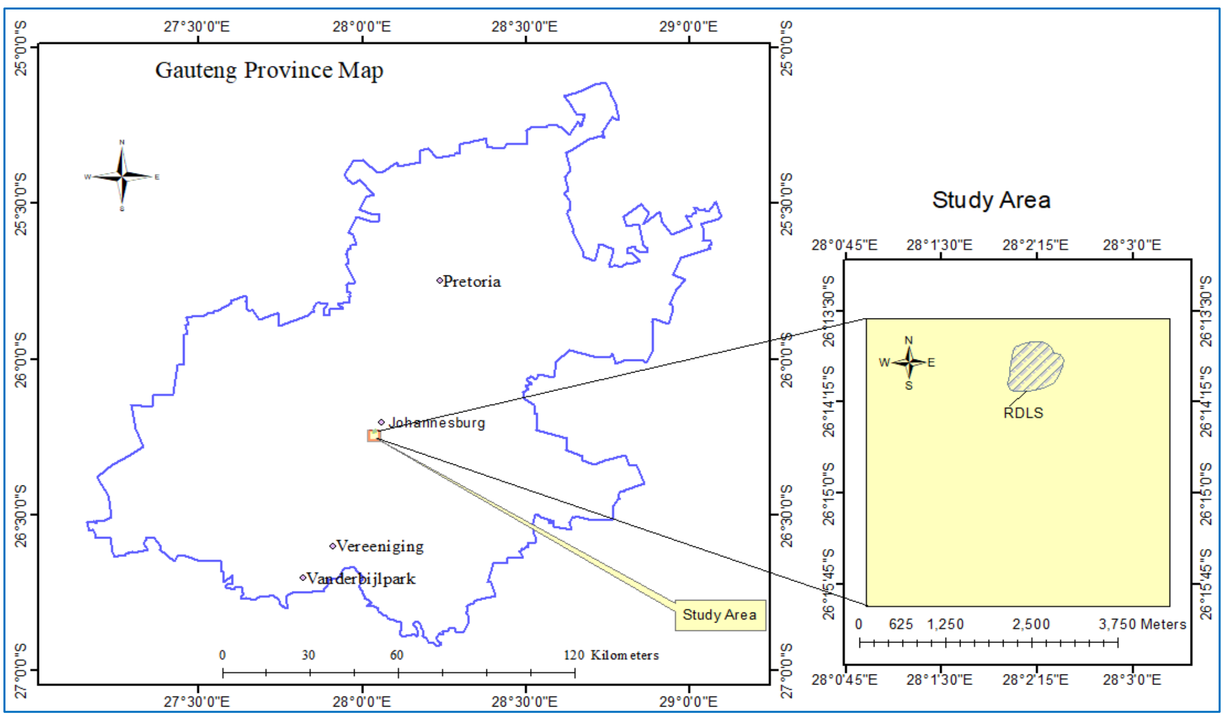

Fig. 1: Location of study area (author)

2.2. Groundwater flow model construction

Groundwater flow (hereafter flow) modelling of the RDL site was performed using Visual MODFLOW Flex Version 8 (VMOD Flex) [36]. The MODFLOW-NWT [37] numerical engine was used to solve the general

JDFEWS 5 (2): 65 - 82, 2024
ISSN 2709-4529

governing equations of the groundwater flow problems. The conceptual modelling approach translated multiple numerical models from a single conceptual model.

2.2.1. Model set up

The extent of the model domain was set to 2800 m × 3600 m × 40 m in the X, Y, and Z dimensions, respectively. The grid discretisation used was a MODFLOW finite difference grid of 144 rows and 112 columns, resulting in 16128 active model cells with a grid spacing of 25 m along the rows and 25 m along the columns. Based on the studies [34][38] and borehole lithology data obtained from the Department of Water and Sanitation (DWS), the thickness of the model domain was set to 40 m comprising three hydrogeological units: sandy loam, sandy clay loam, and fractured rocks—initially, the flow model comprised of the three hydrogeological units mentioned above. However, owing to variations in the groundwater heads in the cells of layer one, the initial heads of some cells in layer one fell below the bottom. MODFLOW-2005 and its Newton–Raphson formulation do not accept that the initial head surface is lower than the bottom of layer one. Therefore, we merged layers one and two into a single layer with reasonably averaged hydraulic properties.

2.2.2. Input parameters and boundary conditions

Input parameters for the flow model consisted of longitudinal, transverse, and vertical hydraulic conductivities (Kx, Ky, and Kz), specific storage (Ss), specific yield (Sy), total porosity (Tp), effective porosity (Ep), and boundary and initial conditions. The flow model contained three boundary conditions and one initial condition: constant Head (CHD), no flow, recharge boundary condition, and initial head condition. The flow model input parameter values and the boundary and initial conditions are listed in Table 1.

Table 1. Flow model input parameters and boundary conditions.

Input parameters	**Parameter value**		**Sources**	
	Layer one	Layer two		
Kx	3.64 x10^{-6} m/s to 1.23 x10^{-5} m/s	9.838 x10^{-6} m/s	[38][39] and borehole lithology	
Ky	3.64 x10^{-6} m/s to 1.23 x10^{-5} m/s	9.838 x10^{-6} m/s	Ky = Kx	
Kz	3.64 x10^{-6} m/s to 1.23 x10^{-5} m/s	9.838 x10^{-7} m/s	Kz = 0.1 x Kx	
Ss	0.0059167 m^{-1} to 0.0265 m^{-1}	0.0065 m^{-1}	Estimated from other parameters	
Sy	0.1065 to 0.053	0.13 or 13%	Estimated parameter	
Tp	0.3 to 0.33	0.18	[38][39]	
Ep	0.25 to 0.26	0.14	[38][39]	
Simulation time in days		9855 days starting from 01/01/1998 to 01/01/2025		
Boundary conditions	CHD	Northern, Southern, and Eastern sides	Same as layer one	Estimated based on initial heads and topography
	No flow	Western and Bottom boundaries	Same as layer one	Assumed
	Recharge	53 to 60 mm annually	Model top	[34]
Initial head condition		Interpolated from water level data obtained from DWS		
Ground surface/model top		Created from the 30 m Shuttle Radar Topography Mission (SRTM) Global DEM from USGS		

JDFEWS 5 (2): 65 - 82, 2024
ISSN 2709-4529

2.2.3. Sensitivity analysis

Sensitivity analysis (SA) is often performed before calibrating and validating the groundwater flow model. In this study, the flow model input parameters and boundary heads were individually increased or decreased to evaluate which parameters significantly impacted the model output (sensitive parameters) and which parameters had no impact on the model output (non-sensitive parameters). Parameter Estimation software (PEST) [23] Version 12.3.1, a VMOD-Flex software component, was used to determine the sensitive parameters of the flow model. Several flow simulation runs were conducted using MODFLOW-NWT with an upstream weighting package (UPW). Then, the sensitive parameters were used in the calibration process of the groundwater flow model.

2.2.4. Calibration and validation

The flow model was calibrated to ensure that the model used for the simulations accurately represented the actual site conditions and produced reasonable results. The most sensitive parameters identified in the sensitivity analysis were used to calibrate the flow model.

Groundwater head and concentration observation data obtained from the DWS were utilised in the calibration process. The borehole data obtained from the DWS contained no production (sink) or injection (source) wells in the model domain. Therefore, there was no well boundary condition defined for the flow model. However, seven observation boreholes recorded water level data on two dates. The seven groundwater level observations listed in Table 2 are the only head observations available in the study area of 10.08 km^2. The head measurements (Gs_5 to Gs_{12}) were used to calibrate the flow model, and (BH-1 and BH-2) were used to validate the flow model.

Table 2. Groundwater head observations used for calibration and validation.

Well Id	X-Coordinate	Y-Coordinate	Elevation (m)	Well bottom	Logger Id	Logger Elevation	Observation time (day)	Observed Head (m)
Gs_5	604294.5667	7098455.676	1708	1680	L5	1688	1095.00	1697.8
Gs_8	603222.4399	7096925.736	1730	1665	L8	1700.4	1095.00	1710.4
Gs_9	603922.1007	7096982.165	1739	1719	L9	1721.2	1095.00	1729.2
Gs_{10}	604141.0464	7098247.565	1707	1687	L10	1689	1095.00	1697
Gs_{12}	603785.2067	7097100.675	1735	1605	L12	1698.69	1095.00	1721.76
BH-1	603754.4359	7097710.576	1715	1695	A1	1700	8907.00	1708.5
BH-2	603096.2822	7097941.353	1708	1688	A2	1690.2	8907.00	1698.2

Source: Wells Gs_5-Gs_{12} (DWS); BH-1 and BH-2 [40].

2.3. Contaminant transport model construction

Contaminant transport modelling of the RDL was conducted using numerical engines built within the software VMOD-Flex-8, such as the MT3DMS. Using the software's graphical user interface (GUI), the output data of the MODFLOW-NWT (flow model) were incorporated into the construction of the contaminant transport model (CTM). The developed CTM was an advection-dispersion-dominated model with no retardation (sorption) or reaction.

Journal of Digital Food, Energy & Water Systems [JD-FEWS]

JDFEWS 5 (2): 65 - 82, 2024
ISSN 2709-4529

2.3.1 Input parameters and boundary conditions

A constant concentration boundary condition was assigned to add a contaminant source as a point source where the heavy metals measured in the study of [40] continuously percolate from the RDL. Table 3 lists the input parameters, boundary conditions, and initial conditions for the transport model.

Table 3. Transport model input parameters.

Model parameters		Unit	Value
Bulk densities for layers one and two [39].	Sandy loam-sandy clay loam	Kg/m^3	1600
	Fractured sandy shale-		2600
Effective porosity (Ep) [39].	Layer one	--	0.25
	Layer two		0.14
Longitudinal dispersivity [41]. α_L	Layer one	m	7
	Layer two		2
Transverse dispersivity α_{TH} and α_{TV}	Layer one	m	α_{TH}/α_L=0.1 α_{TV}/α_L=0.01
	Layer two		
Source concentrations of the CTM species are assigned as a constant concentration boundary [40].	Aluminium (Al)	mg/L	1.49
	Cadmium (Cd)		0.00141
	Manganese (Mn)		10
	Lead (Pb)		16.6
Initial condition/initial concentrations	Applied to the whole model	mg/L	0

2.3.2. Calibration and validation

Eight concentrations of BH-2 and BH-H (Table 4) were used to calibrate the transport model. The calibration parameters used were longitudinal and transverse dispersivities, which were manually determined because the VMOD Flex-8 does not support the automatic calibration of any transport parameters.

The observed concentrations of BH-1 and BH-3 listed in Table 4 were compared to their simulated counterparts to validate the CTM. The CTM validation run contained the original unaltered calibrated validated flow model and the calibrated transport model. The concentration observations of BH-1, BH-2, and BH-3 were collected by [40]. In contrast, the observations of the BH-H were downloaded from the DWS's National Groundwater Archive (NGA).

JDFEWS 5 (2): 65 - 82, 2024
ISSN 2709-4529

Table 4. Heavy metal concentration observations used for CTM calibration and validation.

Well Id	X (m)	Y (m)	Elevation (m)	Well bottom	Logger Id	Logger Z	Chemical	Observation Time (day)	Concentration (mg/L)
BH-1	603754.43	7097710.5	1715	1695	A1	1700	Al	8907	0.00141
BH-1	603754.43	7097710.5	1715	1695	A1	1700	Cd	8907	0.00141
BH-1	603754.43	7097710.5	1715	1695	A1	1700	Pb	8907	5
BH-1	603754.43	7097710.5	1715	1695	A1	1700	Mn	8907	9.4
BH-2	603096.28	7097941.3	1708	1688	A2	1690.2	Al	8907	0.00141
BH-2	603096.28	7097941.3	1708	1688	A2	1690.2	Cd	8907	0.00141
BH-2	603096.28	7097941.3	1708	1688	A2	1690.2	Pb	8907	3.23
BH-2	603096.28	7097941.3	1708	1688	A2	1690.2	Mn	8907	2.7
BH-3	604960.51	7095096.9	1778	1741	A3	1747	Al	8907	0.00141
BH-3	604960.51	7095096.9	1778	1741	A3	1747	Mn	8907	0.0707
BH-3	604960.51	7095096.9	1778	1741	A3	1747	Pb	8907	0.65
BH-3	604960.51	7095096.9	1778	1741	A3	1747	Cd	8907	0.00141
BH-H	604158.51	7098456.5	1708	1680	A-H	1684	Al	553.5	0.048
BH-H	604158.51	7098456.5	1708	1680	A-H	1684	Mn	553.5	3.254
BH-H	604158.51	7098456.5	1708	1680	A-H	1684	Pb	553.5	0.008
BH-H	604158.51	7098456.5	1708	1680	A-H	1684	Cd	553.5	0.005

Source: BH-1, BH-2, and BH-3 [40]; BH-H (DWS).

The residuals between the observed and simulated head and concentration values were used to calculate the calibration and validation statistics [42][43] such as (i) Mean Error (ME), (ii) Root Mean Square Error (RMS), and (iii) normalised root mean squared error (NRMS), as indicated in the following equations:

$$\text{ME} = \frac{1}{n}\sum_{i=1}^{n} (Xo - Xs)i \qquad 1$$

Where;
ME is the mean of the difference between the observed value (Xo) and the simulated value (Xs).
n is the number of calibration or validation measurements

$$\text{RMS} = \left[\frac{1}{n}\sum_{i=1}^{n} (Xo - Xs)i^2\right]^{0.5} \qquad 2$$

Where;
RMS is the square root of the average squared difference between (Xo) and (Xs)

$$\text{NRMS} = \frac{\text{RMS}}{(Xo)max - (Xo)min} \qquad 3$$

Journal of Digital Food, Energy & Water Systems [JD-FEWS]

JDFEWS 5 (2): 65 - 82, 2024
ISSN 2709-4529

After the groundwater flow and transport models passed the calibration and validation criteria of a normalised root mean squared error of $\leq$ 10% [43], the CTM was used to perform predictive simulations to forecast the concentrations of Al, Cd, Mn, and Pb in the groundwater for a simulation period of 11680 days, which corresponds to the period between the start date of the simulation (January 1, 1998) to January 1, 2030.

3. Results and Discussion

3.1 Results

The developed groundwater flow model comprised three horizontal surfaces converted into two structural or property zones, representing the two model layers (Figure 2). The initial description of the hydraulic conductivity for layer one, as shown in Table 1, was based on [38] and [39] findings, which align with the borehole lithology data obtained from the DWS. Then, nine hydraulic conductivity zones were created using the available borehole log data and with the help of the kriging interpolation tool of the VMOD-Flex-8. Zone-based hydraulic conductivities (Figure 3) were preferred to better represent the study area's aquifer characteristics.

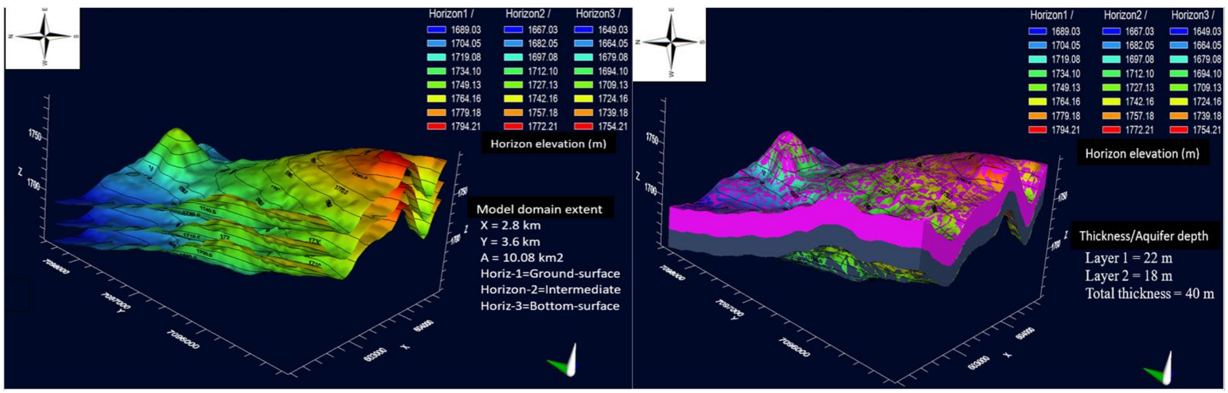

Fig. 2 a): Flow model layer surfaces, **b):** Thickness of the model layers (author).

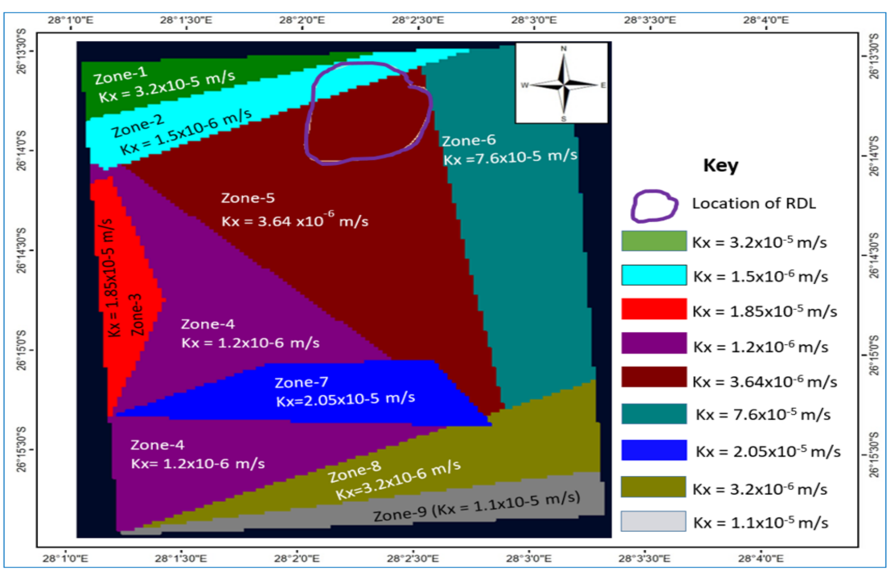

Fig. 3: Zone-based hydraulic conductivities (author).

JDFEWS 5 (2): 65 - 82, 2024
ISSN 2709-4529

Regarding the developed CTM, the flow model grid was refined to focus more on the anticipated contaminant source (RDL). Some studies followed similar flow and transport model construction procedures, such as the study of [24] on modelling the Atlantis aquifer of the industrial town of Atlantis, South Africa, and the study of [26] on contaminant transport modelling of a sewage farm located in south Madurai, Tamil Nadu, India.

3.1.1 Sensitivity analysis

Flow model

A parameter sensitivity analysis was performed before model calibration to determine the sensitive parameters to be included in the model calibration process. In the sensitivity analysis, the effect of adjusting the flow model input parameters, such as hydraulic conductivity components, on the match or goodness of fit between the simulated and observed heads was quantified using the PEST component of the VMOD-Flex-8. The measurement of the sensitivity analysis was based on calculating the ratio of the percentage change in output values divided by the percentage change in input values. In this case, it was found that the horizontal (Kx) and vertical (Kz) hydraulic conductivities were influential parameters in the match between the simulated and observed heads; hence, the model was sensitive to these input parameters. A total of 72 pilot points of Kx and Kz (36 pilot points and one parameter group for each) were defined with fixed hydraulic conductivity values deduced from borehole lithology data obtained from the DWS. The pilot points were spatial points in which the initial parameter values were specified, and the PEST software iteratively estimated the best hydraulic conductivity values based on these designated points (Figure 4). The X-axis shows the parameter group (pg) and pilot-point numbers from pg1-1 to pg2-72, whereas the Y-axis shows the parameter sensitivity coefficients. The pilot-point approach to describing aquifer characteristics often outperforms the zonation technique [44]. However, the zonation technique is more reliable than assigning a single parameter value to an entire aquifer system that can be abruptly heterogeneous.

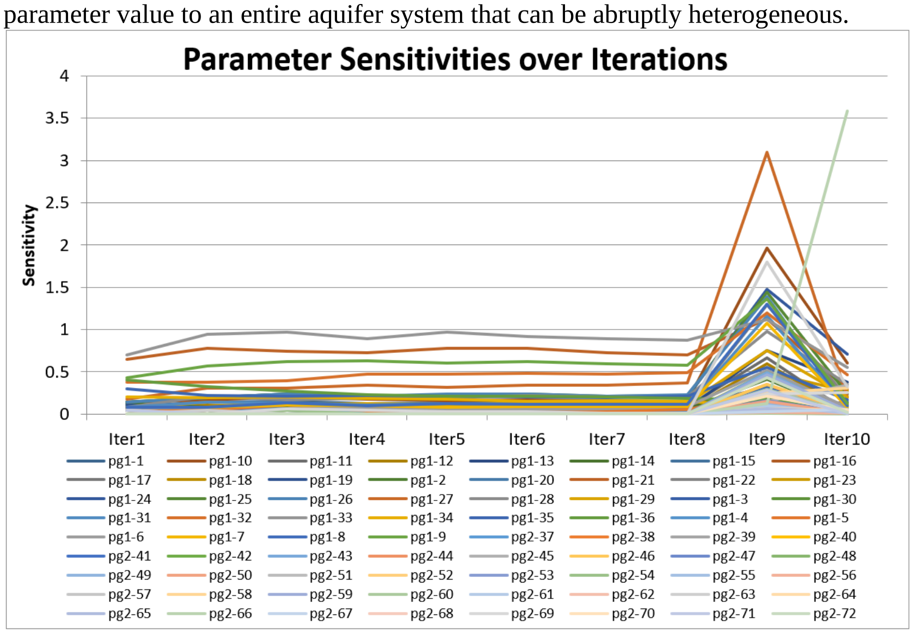

Fig. 4: Kx and Kz pilot-point sensitivities generated by PEST software.

Transport model

Because the automated parameter estimation software (PEST) was not supported in the VMOD-Flex-8 for estimating the transport parameters, manually determining the transport model's sensitive parameters was inevitable. By trial and error, it was found that longitudinal and transverse (horizontal transverse and vertical transverse)

Journal of Digital Food, Energy & Water Systems [JD-FEWS]

JDFEWS 5 (2): 65 - 82, 2024
ISSN 2709-4529

dispersivities were the important influential parameters for calibrating the contaminant transport model. This indicates that these dispersivity parameters are important in predicting the spread of contaminants in groundwater.

3.1.2. Calibration and validation

Flow model

To objectively quantify the goodness-of-fit between the simulated and observed heads, model calibration statistics (calibration criteria), such as the mean error (ME) of the estimates described in equation (1), the root mean squared error (RMS) equation (2), and the normalised root mean squared error (NRMS) equation (3), were calculated. The steady-state groundwater flow model was calibrated against the five head observation wells in Table 2. The calibration result (Figure 5) was considered acceptable according to the commonly used model calibration criterion of an NRMS of less than or equal to 10% [43].

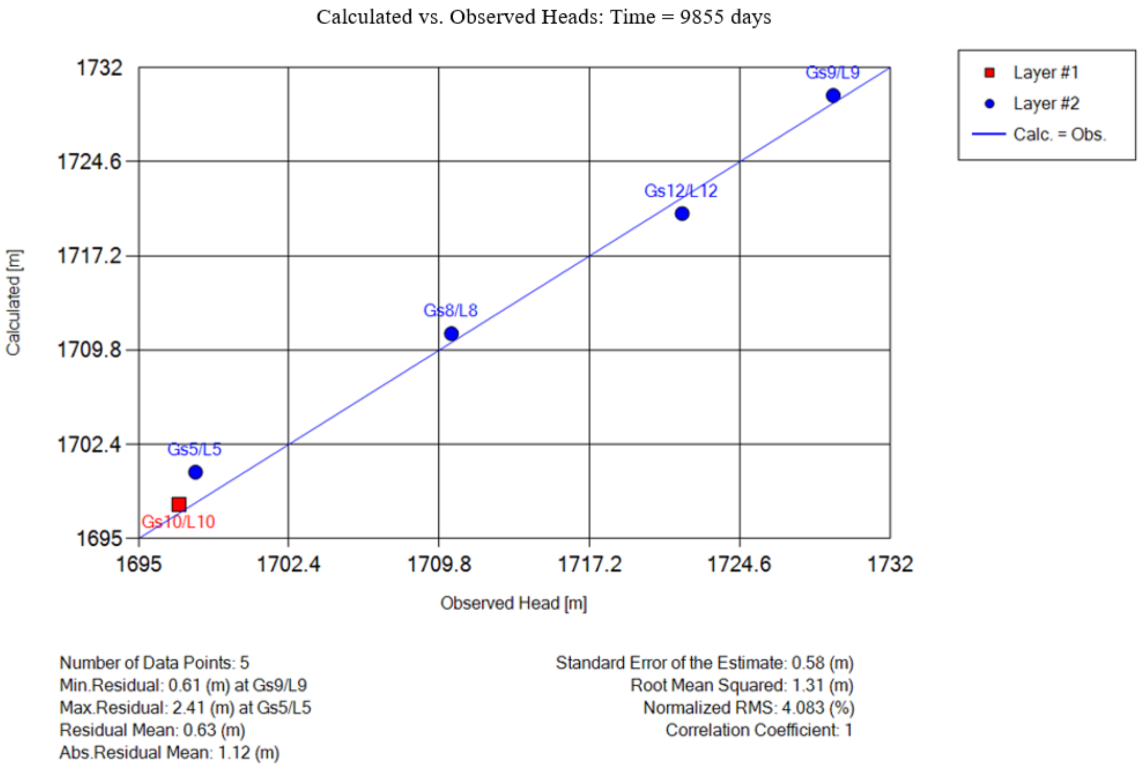

Fig. 5: Calibration curve between calculated and observed heads.

Head observations BH-1 and BH-2 (Table 2), measured on May 24 2022, were used to validate the groundwater flow model. The study performed this measurement using a Solinst TLC meter model 107 (Solinst Canada Ltd) by the study [40].

Validating the groundwater flow model followed the same criteria as the model calibration, requiring an NRMS of less than or equal to 10% [42][43]. The calibrated flow model was validated against the two head observations (BH-1 and BH-2) without adjusting a single flow model parameter because this makes the model uncalibrated. The result of flow model validation is presented in Table 5.

JDFEWS 5 (2): 65 - 82, 2024
ISSN 2709-4529

Table 5. Flow model validation statistics.

Criteria	Results
Number of observations	2
Minimum residual	0 m
Maximum residual	5.25 m
Residual mean	2.62 m
Absolute residual	2.63 m
Standard error	1.25 m
Root mean squared error	3.71 m
Normalised root mean squared error	0.22%
Correlation coefficient	1

Although the number of data points (observations) used is small, the flow model validation statistics presented in Table 5 indicate that the model has high accuracy and reliability.

Transport model

To calibrate the CTM, initial parameter values for longitudinal, horizontal transverse, and vertical transverse dispersivities for model layer one were set at 5m, 0.5m, and 0.05m, respectively, and 2m, 0.2m, and 0.02m for the dispersivities, of layer two respectively. The CTM calibration parameters were adjusted manually more than 50 times better to match the heavy metals' simulated and observed concentrations. The concentration observations BH-2 and BH-H containing eight measurements of Al, Cd, Mn, and Pb were used to calibrate the transport model. Only four concentration observation points were available in the study area, each containing four concentration measurements. Two observation points (BH-2 and BH-H) were used for calibration, and the other (BH-1 and BH-3) for validation.

The transport model was run for a simulation period of 9125 days (25 years) with transport steps of 1, 365, 1500, 3000, 7000, and 9125 days. The PEST tool uses the concentration residuals (Table 6a) to calculate the calibration objective function phi (Φ), the sum of the weighted, squared, and simulated-to-observed concentration discrepancies. The transport model calibration criteria were satisfied; the results are listed in Table 6b.

Table 6a. Concentration residuals.

Observation point	Parameter	Observed (mg/L)	Simulated (mg/L)	Residuals (mg/L)
BH-2	Al	0.00141	0.0865	0.08509
	Cd	0.00141	0.001	-0.00041
	Mn	2.7	2.809	0.109
	Pb	3.23	3.2	-0.03
BH-H	Al	0.048	0.05	0.002
	Cd	0.005	0.0043	-0.0007
	Mn	3.254	2.264	-0.99
	Pb	0.008	0.0077	-0.0003

JDFEWS 5 (2): 65 - 82, 2024
ISSN 2709-4529

Table 6b. Transport model calibration statistics.

Criteria	Results
Number of observations	8
Minimum residual	0.0003 mg/L
Maximum residual	-0.99 mg/L
Residual mean	-0.103 mg/L
Absolute residual	1.2175mg/L
Standard error	0.67 mg/L
Root mean squared error	0.292 mg/L
Normalised root mean squared error	8.977%
Correlation coefficient	0.97

A new set of concentration observations is required to validate the transport model. Borehole one (BH-1) and borehole three (BH-3) concentration observations were used to validate the CTM. Transport model validation (verification) followed the same criteria as the model calibration, requiring the NRMS to be less than or equal to 10%. Table 7 presents the result of the CTM validation.

Table 7. Transport model validation statistics.

Criteria	Results
Number of observations	8
Minimum residual	0 mg/L
Maximum residual	5.62 mg/L
Residual mean	0.34 mg/L
Absolute residual	1.09 mg/L
Standard error	0.81 mg/L
Root mean squared error	2.16 mg/L
Normalised root mean squared error	9.98%
Correlation coefficient	0.91

3.2. Discussion of the Results

The developed groundwater flow and transport models met their calibration and validation criteria [25][42][43]. Therefore, these models are reliable and effective in predicting groundwater contamination in the study area.

The transport simulation period of 9125 days, starting from January 1, 1998, accommodated April 20, 1999, metal concentration observations used for CTM calibration and May 24, 2022, observations used for CTM validation. Notably, the 1999 groundwater quality observation was the only relevant historical observation available in the NGA. The results of the transport simulation showed that the heavy metal plume migration from the RDL was slow and reached the observation boreholes on day 7000 (Figure 6a). Notably, this study assumed that the model domain was initially free from heavy metal contamination and that the landfill started leaking heavy metals at the start of the simulation period. On day 7000, the leachate plume reached BH-2 and moved in the northern direction of BH-H. On day 9125, corresponding to January 1, 2023, a plume containing Mn and Pb concentrations of 4.28 mg/L and 6.85 mg/L crossed the model boundary in the northern direction of the RDL. The simulation result of the heavy metal concentrations is in line with the findings of [40], which indicated a possibility of leachate plume migration towards these boreholes. Though the study of [40] used the same observation points as shown in Figure 6b, that study aimed to assess the spatial correlation between groundwater quality of boreholes (BH-1, BH-2, BH-3, and BH-H) in terms of heavy metal concentration and the distance to the RDL.

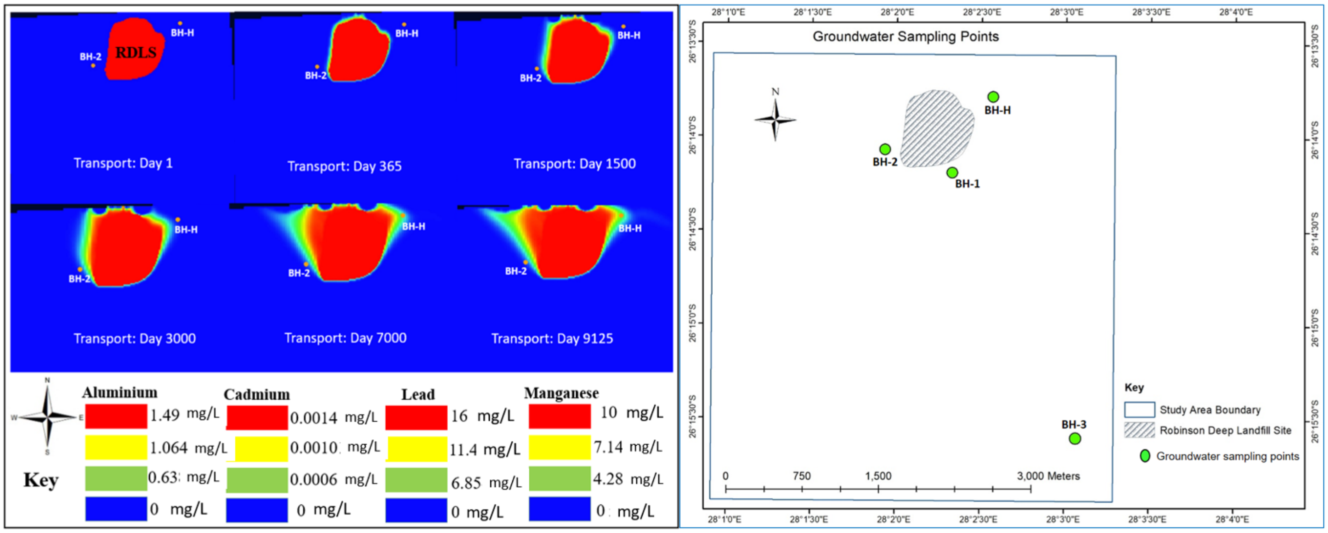

Fig. 6a): Plume migration from day 1 to day 9125, **b):** Observation points [40].

Both the simulated concentrations of Mn and Pb in the groundwater of the boreholes (BH-1, BH-2, BH-3, and BH-H) and the heavy metal concentrations measured by [40] exceed the local water quality guidelines such as the Department of Water Affairs and Forestry [45], the South African National Standards (SANS) for drinking water quality guidelines [46], and international guidelines such as the World Health Organization [47]. As a result, it is evident that the RDL currently threatens groundwater quality in the study area, particularly in areas north of the RDL. Notably, the RDL operates under several permits and licenses required under various South African Environmental laws. The landfill managing company, Pikitup, must submit groundwater monitoring data twice a year to the Department of Water and Sanitation.

The area in the southern direction of the RDL is likely not affected by groundwater contamination due to a leachate plume that comes from the RDL. This is because the southern direction of the RDL is generally upgradient and opposes the direction of the groundwater flow in the study area; moreover, the CTM showed that the dominant transport mechanism in the study area is advection, and mass transport by dispersion has a minimum effect unless a simulation period of more than a century is forecasted. In this study, mass transport by dispersion could not overcome the dominant transport, which is advective transport driven by the bulk motion of flowing groundwater.

The calibrated validated CTM was run one last time for a simulation period of 11,680 days. This simulation period corresponds to 32 years from 01/01/1998 to 01/01/2030, and it was intended to predict how the plume of contaminants from the RDL spreads and the resulting groundwater contamination. The predictive simulation showed that a plume of contaminated groundwater from the RDL spreads toward the BH-H. According to the result of the predictive simulation, the leachate plume or highly contaminated groundwater will not be able to reach boreholes BH-1 and BH-3 in the current simulation period until 2030. However, highly polluted groundwater, which has elevated concentrations of Pb and Mn, was predicted at the location of BH-H, as Figure 7 depicts.

Journal of Digital Food, Energy & Water Systems [JD-FEWS]

JDFEWS 5 (2): 65 - 82, 2024
ISSN 2709-4529

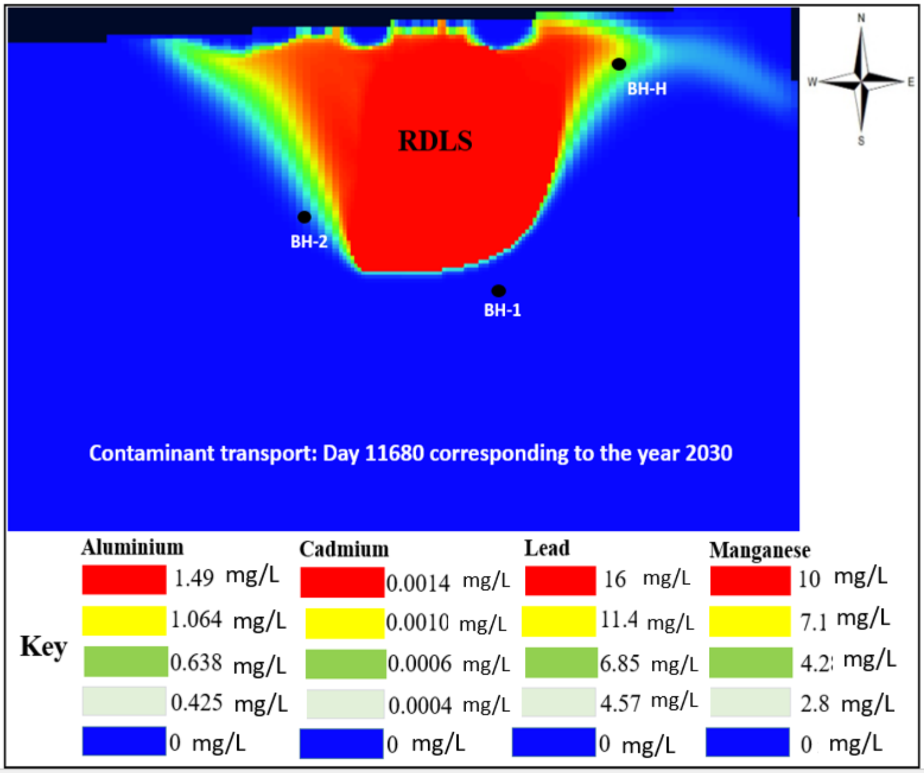

Fig. 7: Predictive simulation result showing plume spread.

The groundwater quality of the BH-H is predicted to have heavy metal concentrations of 0.638 mg/L, 0.0006 mg/L, 6.85 mg/L, and 4.2 mg/L for Al, Cd, Pb, and Mn, respectively. All other predicted concentrations at BH-H were above the permissible limit except for the Cd concentration. Figure 8 (a-d) shows predicted concentrations of the heavy metals versus the time graph of BH-H from day one, from January 1 1998 to day 11680, to January 1 2030.

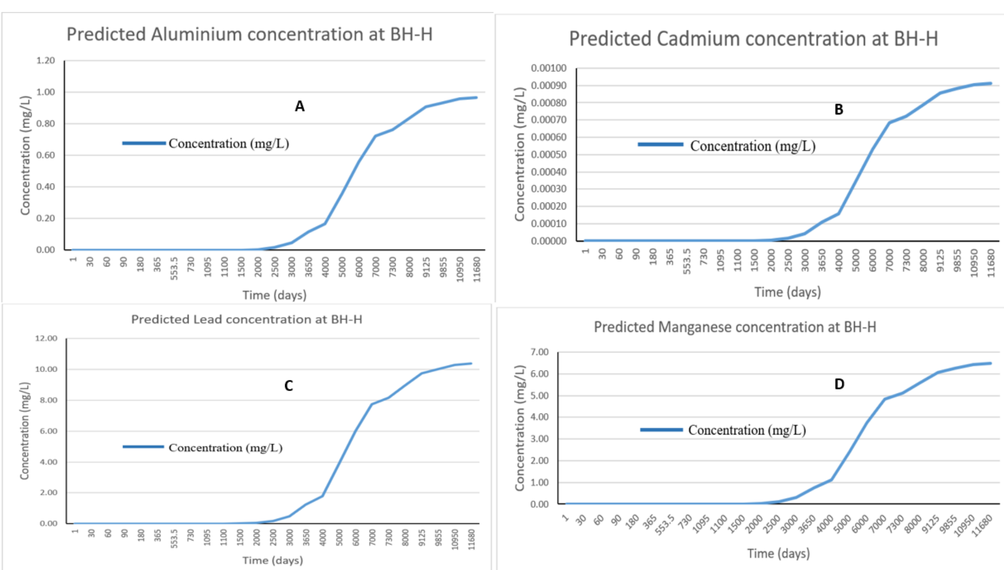

Fig. 8: Predicted heavy metal concentrations versus time graph for the BH-H.

JDFEWS 5 (2): 65 - 82, 2024
ISSN 2709-4529

Although the rate of contaminant migration in underground environments is spatially and temporally variable, the findings of this study align well with other studies on contaminant transport modelling. The studies [24] and [26] found a contaminant plume migration rate in the range of 10m to 300m per year, while the current study found a plume migration rate of 12m to 60m per year. The migration rate of heavy metals observed in this study is slow, indicating the need for long-term groundwater monitoring strategies. The developed CTM's predictive simulations highlight the potential risks of heavy metal contamination, particularly Mn and Pb, which are projected to exceed permissible limits by 2030. Furthermore, the study's emphasis on the need for post-closure care and monitoring facilities for the RDL echoes the recommendations of [9] and [10], highlighting the importance of continuous monitoring to protect groundwater from landfill-related contamination. Finally, Policymakers can utilise these findings to formulate regulations that mandate groundwater monitoring practices for landfill sites nearing closure.

4. Conclusion

The overall objective of this study was to establish a calibrated, validated groundwater flow and contaminant transport model for the Robinson Deep landfill area located in Johannesburg, South, to predict groundwater quality in and around the RDL. The transport modelling results showed that the heavy metals released at the RLD moved at 60 m/year to reach the BH-H and a rate of 12 m/year to reach BH-2. However, the leachate plume or the highly contaminated groundwater could not reach boreholes BH-1 and BH-3, and generally, the leachate leaked by the RDL did not travel southwards.

The predictive simulation shows that in 2030, the concentrations of Pb, Mn, Al, and Cd in the groundwater of the BH-H can reach up to 6.85 mg/L, 4.2 mg/L, 0.638 mg/L, and 0.0006mg/L respectively. All other predicted concentrations at BH-H were above the permissible limit except for the Cd concentration.

In summary, the results indicate that the RDL threatens the groundwater quality of its proximate areas, particularly in the northern direction of the landfill site. It is expected that the RDL will close; however, even after closure, it may adversely affect the groundwater quality of the proximate areas soon.

One of the limitations of this study was limited funding, which did not allow the research to obtain more data to cover the complexities of groundwater-leachate interactions in the study area. However, the findings of this study may support the post-closure care of the landfill site so that management can ensure that this landfill safely stabilises without damaging the groundwater. In addition, because the landfill is on the verge of closure, post-closure groundwater monitoring facilities should be installed, and future groundwater flow and transport modelling studies should focus more on the northern direction of the landfill, where the present study has predicted elevated concentrations of heavy metals. Further, it is recommended that precautionary preventive measures be implemented to mitigate possible contamination of groundwater in the northern areas of the landfill.

Declaration of competing interests

"We declare that there are no conflicts of interest to disclose."

Acknowledgements

The Vaal University of Technology is acknowledged for providing financial support and purchasing Visual MODFLOW Flex Pro.

JDFEWS 5 (2): 65 - 82, 2024
ISSN 2709-4529

References

[1] D. Sheng, X. Meng, X. Wen, J. Wu, H. Yu, and M. Wu, Contamination characteristics, source identification, and source-specific health risks of heavy metal(loid)s in groundwater of an arid oasis region in Northwest China, Sci. Total Environ. 2022;841:156733. https://doi.org/10.1016/j.scitotenv.2022.156733
[2] D. Abiriga, l. Vestgarden, H. Klempe, Groundwater contamination from a municipal landfill: effect of age, landfill closure, and season on groundwater chemistry. Sci. Total Environ. 2020;737:140307. https://doi.org/10.1016/j.scitotenv.2020.140307
[3] P. Ravenscroft, L. Lytton, Seeing the invisible: A strategic report on groundwater quality. Report no. 169674. Washington, DC: World Bank; 2022.
[4] United Nations, The United Nations World Water Development Report 2024: Water for Prosperity and Peace. UNESCO, Paris. https://doi.org/10.18356/9789210050000
[5] I.V. Sibiya, O.I. Olukunle, Okonkwo, Seasonal variations and the influence of geomembrane liners on the levels of PBDES in landfill leachates, sediment and groundwater in Gauteng Province, South Africa. Emerg. Contam. 2017;3(2):76–84. https://doi.org/10.1016/j.emcon.2017.05.002
[6] J.N. Edokpayi, O.S. Durowoju, J.O. Odiyo, Assessment of heavy metals in landfill leachate: A case study of Thohoyandou landfill, Limpopo Province, South Africa. Heavy Met. 2018;16:214–227. https://doi.org/10.5772/intechopen.74009
[7] V. Nevondo, A.P. Daso, O.J. Okonkwo, T. Malehase, Leachate seepage from landfill: a source of groundwater mercury contamination in South Africa. Water Sa. 2019;45(2):225-231. https://hdl.handle.net/10520/EJC-15974e82c8
[8] I. Sibiya, G. Poma, M. Cuykx, A. Covaci, P. Adegbenro, J. Okonkwo, Targeted and non-target screening of persistent organic pollutants and organophosphorus flame retardants in leachate and sediment from landfill sites in Gauteng Province, South Africa. Sci. Total Environ. 2019;653:1231–1239. https://doi.org/10.1016/j.scitotenv.2018.10.356
[9] R. Makhadi, S.A. Oke, O.O. Ololade, The influence of non-engineered municipal landfills on groundwater chemistry and quality in Bloemfontein, South Africa. Molecules. 2020;25(23):5599. https://doi.org/10.3390/molecules25235599
[10] S. Mepaiyeda, K. Madi, O. Gwavava, O. Baiyegunhi, Geological and geophysical assessment of groundwater contamination at the Roundhill landfill site, Berlin, Eastern Cape, South Africa. Heliyon. 2020;6(7):E04249. https://doi.org/10.1016/j.heliyon.2020.e04249
[11] T.K. Boateng, F. Opoku, O. Akoto, Heavy metal contamination assessment of groundwater quality: A case study of Oti landfill site, Kumasi. Appl. Water Sci. 2019;9:33. https://doi.org/10.1007/s13201-019-0915-y
[12] Y. El-mouine, Amal el H, Moad M, Vincent V, Hasna Y, Houria D. Groundwater contamination due to landfill leachate—A case study of Tadla Plain. Environ. Sci. Proc. 2020;16(1):53. https://doi.org/10.3390/environsciproc2022016053
[13] L. Lindamulla, Nanayakkara N, Othman M, Jinadasa S, Herath G, Jegatheesan V. Municipal solid waste landfill leachate characteristics and their treatment options in tropical countries. Curr. Pollut. Rep. 2022;8:273–287. https://doi.org/10.1007/s40726-022-00222-x
[14] A. Wdowczyk, szymańska-pulikowska A. Analysis of the possibility of conducting a comprehensive assessment of landfill leachate contamination using physicochemical indicators and toxicity test. Ecotoxicol. Environ. Saf. 2021;221:112434. https://doi.org/10.1016/j.ecoenv.2021.112434
[15] C. Teng, Chen W. Technologies for the treatment of emerging contaminants in landfill leachate. Curr. Opin. Environ. Sci. Health. 2023;31:100409. https://doi.org/10.1016/j.coesh.2022.100409
[16] M. Bakker, Post V. Analytical groundwater modelling—Theory and applications using Python. London, UK. Taylor & Francis Group; 2022.
[17] A.M. Gahala, Bristow ELD, Sharpe JB, Metcalf BG, Matson LA. Simulation of groundwater and surface-water interaction and lake resiliency at Crystal Lake, City of Crystal Lake, Illinois. Reston, VA: USGS; 2024. https://doi.org/10.3133/sir20245007
[18] C.P. Kumar, An overview of commonly used groundwater modelling software. Int. J. Adv Res. Sci. Eng. Technol. 2019; 6(1):7854-7865.
[19] C.D. Langevin, Hughes JD, Banta ER, Niswonger RG, Panday S, Provost AM. Documentation for the MODFLOW 6 groundwater flow model. Reston, VA: USGS; 2017. https://doi.org/10.3133/tm6A55
[20] C.P. Kumar, modelling of groundwater flow and data requirements. Int. J. Mod. Sci. Eng. Technol. 2015;2(2):18-27.
[21] M.G. Mcdonald, Harbaugh AW. A modular three-dimensional finite-difference groundwater flow model. USGS. Book 6, Chapter A1:586; 1988. https://doi.org/10.3133/twri06A1
[22] S. Rwanga, Ndambuki J. Solving groundwater problems fraught with uncertain recharge: An application to Central Limpopo, South Africa. Groundw. sustain. dev. 2020;10:100305. https://doi.org/10.1016/j.gsd.2019.100305
[23] J. Doherty, Calibration and uncertainty analysis for complex environmental models. Brisbane, Australia: Watermark Numerical Computing; 2015. https://doi.org/10.1111/gwat.12360
[24] N. Jovanovic, Bugan RD, Tredoux G, Israel S, BIshop R, Marinus V. Hydrogeological modelling of the Atlantis aquifer for management support to the Atlantis Water Supply Scheme. Water S.A. 2017;43(1):122-138. https://doi.org/10.4314/wsa.v43i1.15

JDFEWS 5 (2): 65 - 82, 2024
ISSN 2709-4529

[25] C. Zheng, Wang PP. MT3DMS: A modular three-dimensional multispecies transport model for simulation of advection, dispersion, and chemical reactions of contaminants in groundwater systems; documentation and user's guide. Contract report SERDP-99-1. Vicksburg, USA. US Army Corps of Engineers Engineer Research and Development Centre; 1999.
[26] C. Sundararaj, Muthukaruppan K, Mariappan D, Veluswamy K. Groundwater contaminant transport modelling using Visual MODFLOW: A case study of corporation sewage farm in South Madurai, Tamil Nadu, India. Arab. J. Geosci. 2022;15(18):1538. https://doi.org/10.1007/s12517-022-10804-0
[27] Akinsulie OO. Material flow analysis on a landfill site in Johannesburg. Dissertation (M.Sc.). Johannesburg: The University of the Witwatersrand; 2016.
[28] Musekiwa C, Majola K. Groundwater vulnerability map for South Africa. S.A. J. Geomat. 2013;2(2):152–162.
[29] Barnard HC. Hydrogeological map of Johannesburg 2526 (1:500 000). Department of Water Affairs and Forestry, Pretoria, Johannesburg, South Africa; 1999.
[30] Coetzee LE. Geological series 2628 East Rand (1:250000). South African Department of Mineral and Energy Affairs, Pretoria; 1986.
[31] De Beer JH. Geology of Johannesburg, Republic of South Africa. Bulletin of the Association of Engineering Geologists. 1986;23(2):101-137. https://doi.org/10.2113/gseegeosci.xxiii.2.101
[32] Wilkinson KJ. Geological Series 2626 West Rand (1:250000). South African Department of Mineral and Energy Affairs, Pretoria; 1986. Downloadable Material - Council for Geoscience
[33] Johnson MR, Wolmarans LG. Simplified geological map of the Republic of South Africa and the kingdoms of Lesotho and Swaziland. 1:2 000 000. Council for Geoscience, Pretoria; 2008.
[34] Burger M, Vermeulen PD. The groundwater interaction of a deeper lying gold mine and a shallower lying coal mine through the presence of naturally occurring as well as induced preferential flow paths. Presented at: 11th International Mine Water Association Congress–Mine Water–Managing Challenges Conference. Aachen, Germany. IMWA; 2011.63-567.
[35] Mokhahlane LS, Mathoho G, Gomo M, Vermeulen D. Qualitative hydrogeological assessment of vertical connectivity in aquifers surrounding an underground coal gasification site. J. South. Afr. Inst. Min. Metall. 2018;118(10):1047-1052.
[36] Waterloo Hydrogeologic. Visual MODFLOW version 8.0 user's manual-integrated conceptual and numerical groundwater modelling software. Ontario, Canada: Waterloo Hydrogeologic Inc.; 2022. Visual MODFLOW Flex 8.0 Product Release (waterloohydrogeologic.com)
[37] Niswonger RG, Panday S, Motomu I. MODFLOW-NWT, A newton formulation for MODFLOW-2005: US Geological Survey techniques and methods.2011;6–A37:44p. http://pubsdata.usgs.gov/pubs/tm/tm6a37/index.html
[38] Leketa k. Abiye T. Using environmental tracers to characterise groundwater flow mechanisms in the fractured crystalline and karst aquifers in Upper Crocodile River basin, Johannesburg, South Africa. Hydrology. 2021;8(1):50–50. https://www.mdpi.com/2306-5338/8/1/50
[39] Vermaak JJG. Geotechnical and hydrogeological characterization of residual soils in the vadose zone. Thesis (Doctoral). Pretoria: University of Pretoria; 2000. http://hdl.handle.net/2263/30093
[40] Osman OA, Ochieng GM, Rwanga S. Assessment of groundwater quality correlation to proximate landfill leachate: A case study on a selected landfill in Johannesburg, South Africa. [Unpublished manuscript]. Department of Civil Engineering, Vaal University of Technology; 2024.
[41] Xu M. Eckstein Y. Use of weighted least-squares method in evaluation of the relationship between dispersivity and field scale. Groundwater. 1995;33(6):905-908. https://doi.org/10.1111/j.1745-6584.1995.tb00035.x
[42] Khadri SFR. Pande C. Groundwater flow modelling for calibrating steady state using MODFLOW software: A case study of Mahesh River Basin, India. MESE. 2016;2(1):39. https://doi.org/10.1007/s40808-015-0049-7
[43] Shamsi UMS, Koran J. Continuous calibration. JWMM. 2017;25:C414. https://doi.org/10.14796/JWMM.C414
[44] Baalousha HM, Fahs M, Ramasomanana F, Younes A. Effect of pilot-points location on model calibration: Application to the northern karst aquifer of Qatar. Water. 2019;11(4):679. https://doi.org/10.3390/w11040679
[45] DWAF (Department of Water Affairs, South Africa). South African water quality guidelines, volume 1, 2nd edn. Domestic water use. Pretoria, South Africa: Department of Water Affairs and Forestry; 1996.
[46] SABS (South African Bureau of Standards). SANS 241:1 Drinking Water. Pretoria, South Africa: SABS Standards Division; 2015.
[47] WHO (World Health Organization). Guidelines for drinking-water quality: Incorporating the first and second addenda. Geneva, Switzerland: WHO; 2022.